

Reactions between Calcium- and Strontium-Substituted Lanthanum Cobaltite Ceramic Membranes and Calcium Silicate Sealing Materials

Sonia Faaland, Mari-Ann Einarsrud, and Tor Grande*

Department of Chemistry, Norwegian University of Science and Technology,
7491 Trondheim, Norway

Received December 1, 1999. Revised Manuscript Received September 26, 2000

The reaction between Ca- and Sr-substituted LaCoO_3 and $\text{CaSiO}_3/\text{Ca}_2\text{SiO}_4$ has been studied by electron microscopy (SEM and TEM) and X-ray diffraction. The aim was to investigate the chemical stability of these materials as a model system for, respectively, a membrane and a sealing material in dense oxygen-permeable membrane systems. Sintered powder mixtures of the two materials were analyzed to gain information about coexistent phases in the $\text{CaO/SrO-La}_2\text{O}_3\text{-CoO-SiO}_2$ system. The estimated phase composition along the $\text{CaSiO}_3\text{-LaCoO}_3$ line has been worked out. The chemical aspects of glass-ceramic sealing of dense perovskite membranes were studied by making diffusion couples. LaCoO_3 was found to be kinetically more stable to calcium silicate than Ca- and Sr-substituted LaCoO_3 . The results also revealed that Ca_2SiO_4 is a more suitable sealing material than CaSiO_3 , due to lower reactivity. Thus, the stability of the membrane/sealant interface was observed to be quite sensitive to the O:Si ratio of the calcium silicate: $3 < \text{O:Si} < 4$ will give rise to good sealing properties and moderate reactivity to the membrane material. A suitable material is a two-phase material with O:Si close to four, e.g. an orthosilicate glass-ceramic material with small amounts of metasilicate or disilicate glass.

1. Introduction

Dense oxygen-permeable membranes require gastight seals between the membrane and a support. During the bonding process and operation, the sealing materials tend to react with the ceramic membranes to form secondary phases. Some degree of chemical reaction is needed to make the interface between the membrane material and the sealant gastight,¹ but the membrane interface should be stable under operation. The reaction of dense ceramic membranes with sealing materials has not been examined thoroughly in the literature. But the reactivity of $\text{La}_{1-x}\text{Ca}_x\text{CrO}_3$ with silica-based glass materials for solid oxide fuel cells (SOFC) applications has been studied.^{2–4} The formation of secondary phases, such as ZrSiO_4 , Cr_2O_3 , $\text{Ca}_2\text{La}_8(\text{SiO}_4)_6\text{O}_2$, and $\text{Ca}_6\text{La}_4(\text{SiO}_4)_6$, at the interface as well as interdiffusion of cations between the materials will have a negative impact on the SOFC performance.

In this work we have studied a model system for the membrane/sealant interface consisting of $\text{La}_{1-x}\text{M}_x\text{CoO}_3$

($\text{M} = \text{Ca, Sr}; x = 0, 0.2, 0.5$) (LMC) and calcium silicate (CaSiO_3 and Ca_2SiO_4). Potential industrial membranes are supposed to contain La_2O_3 , CaO , and SrO as the more basic oxide constituents and Co as one among two or more transition elements.^{5,6}

Silica-based glasses are potential sealants because their softening temperatures are lower than the operating temperature of the membrane, normally 800–1000 °C.⁵ The glass transition temperature, T_g , for CaSiO_3 is 770 °C;⁷ hence, stress relaxation of the glass will occur at the operating temperature, and CaSiO_3 is a promising sealant. We have chosen to focus on glass-ceramic sealing materials in order to reduce the reactivity expected for a completely amorphous sealant. A desired property of a sealing material is the ability to seal by viscous flow. The viscosity of CaSiO_3 at 1000 °C is $\sim 10^5$ P, extrapolated from data in Mazurin et al.⁸ The viscosity is also lowered by increasing the CaO content in the calcium silicate. Thus, Ca_2SiO_4 is also a promising sealant if complete devitrification is hindered.

The aim of the present investigation is 2-fold. First, important phase relations in the $\text{CaO/SrO-La}_2\text{O}_3\text{-CoO-SiO}_2$ system have been obtained. Second, formation of secondary phases in diffusion couples was analyzed as a function of substitution degree of LaCoO_3 , type of sealing material, and partial pressure of oxygen to gain

* Corresponding author. E-mail: Tor.Grande@chembio.ntnu.no.

(1) Donald, I. *J. Mater. Sci.* **1993**, *28*, 2841.

(2) Horita, T.; Sam, J.-S.; Lee, Y.-K.; Sakai, N.; Kawada, T.; Yokokawa, H.; Dokiya, M. *J. Am. Ceram. Soc.* **1995**, *78*, 7, 1729.

(3) Horita, T.; Sakai, N.; Kawada, T.; Yokokawa, H.; Dokiya, M. *Denki Kagaku* **1993**, *61*, 7, 760.

(4) Yamamoto, T.; Itoh, H.; Mori, M.; Mori, N.; Watanabe, T. *Denki Kagaku* **1996**, *64*, 6, 575.

(5) Balachandran, U.; Dusek, J. T.; Mieville, R. L.; Poeppel, R. B.; Kleefisch, M. S.; Pei, S.; Kobylinski, T. P.; Udovich, C. A.; Bose, A. C. *Appl. Catal. A: Gen.* **1995**, *133*, 19.

(6) Maiya, P. S.; Balachandran, U.; Dusek, J. T.; Mieville, R. L.; Kleefisch, M. S.; Udovich, C. A. *Solid State Ionics* **1997**, *99*, 1.

(7) Shelby, J. E. *J. Appl. Phys.* **1979**, *50*, 12, 8010.

(8) Mazurin, O. V.; Strelins, M. V.; Shavaiko-Shavaikovskaya, T. P. *Handbook of Glass Data, Physical science data 15 A*; Elsevier: Amsterdam, 1983.

knowledge about the sealing of dense ceramic membranes with silica-based sealants. The most suitable sealant system will be proposed.

2. Experimental Procedures

2.1. Sample Preparation. Submicron (0.1–0.5 μm), stoichiometric $\text{La}_{1-x}\text{M}_x\text{CoO}_3$ ($\text{M} = \text{Ca}$ and Sr) powders with $x = 0, 0.2$ and 0.5 were prepared by spray pyrolysis using EDTA as complexing agent.⁹ The composition of the powders was measured by atom scan 16 ICP-AES spectrometry (Thermo Jarrell Ash Corp.), revealing stoichiometric powders. The deviation from nominal composition was less than 1%. The raw powders were calcined in air for 10 h at 900 °C. The two powders with $x = 0.5$ were additionally calcined for 24 h at 950 °C. After calcination, the powders were ball-milled in ethanol for 24 h. According to the X-ray diffraction (XRD) patterns, all powders were single phase. The crystal structure was rhombohedral for all compositions except for 50 mol % Ca or Sr on the La-site, where cubic symmetry was observed.

Calcium metasilicate, CaSiO_3 , was prepared from a stoichiometric mixture of SiO_2 and CaCO_3 (99%, Merck AG). SiO_2 was prepared by a two-step acid/base-catalyzed sol-gel route using tetramethoxysilane (TMOS) as precursor. After preparation the dried gel was crushed before mixing with CaCO_3 . The powder mixture was uniaxially pressed at 90 MPa and fired in air for 36 h at 1400 °C. The pellet was then crushed, once again uniaxially pressed at 90 MPa and fired for 168 h at 1400 °C, obtaining a density of >92% of theoretical with a grain size <20 μm . According to XRD, the CaSiO_3 pellets consist of two polymorphs, cyclowollastonite (main phase) and wollastonite (traces), in addition to residual glass. By thermal etching for 1 h at 1200 °C, the amorphous phase was observed to be situated at grain boundaries.

Calcium orthosilicate, Ca_2SiO_4 powder (>99%, <44 μm), was supplied from Alfa Aesar, a Johnson Matthey company. The structure was monoclinic (β -structure, PDF card 33-302, ICDD 1999). After sedimentation in ethanol, the grain size of the fine fraction was <5 μm . Pellets were uniaxially pressed at 90 MPa and sintered in air at 1600 °C for 60 h, followed by quenching in air. By quenching, dusting¹⁰ was prevented, and the density of the sintered pellets was >90% of theoretical with a grain size <15 μm . XRD reveals that the orthosilicate phase of the sintered pellets has the monoclinic structure (β structure). Only traces of the α -phase, stable at 1600 °C, were observed.

2.2. Reaction Experiment. **2.2.1. Powder Mixture Reaction.** LMC/ CaSiO_3 samples were prepared in the form of powder mixtures, giving a large contact area between the two phases. Mass ratios of 1:1 LMC and CaSiO_3 powders (<7.5 μm) were mixed by dry ball-milling for 5 h using Si_3N_4 balls. In addition, powder mixtures of LaCoO_3 and CaSiO_3 with 22 mol % LaCoO_3 were prepared. The samples were uniaxially pressed at 90 MPa and fired in air and in reducing atmosphere ($p_{\text{O}_2} \sim 10^{-6}$ atm) at 1000–1100 °C for 48–72 h. Similarly LMC/ Ca_2SiO_4 (<5 μm) powder mixtures were prepared and fired in air and in reducing atmosphere at 1200 °C for 72 h.

2.2.2. Diffusion Couple Reaction. For practical reasons diffusion couples of LMC and CaSiO_3 or Ca_2SiO_4 were prepared by the following procedure: The calcium silicate pellets were ground and polished to obtain good contact with the perovskite. A slurry of the perovskite powders was prepared by adding wax (Bronzebinder, TBK Siebdruck Hilfsmittel, Marabu) to the calcined LMC powder in a mass ratio powder:wax = 1:1.25. The LMC films of 1 cm^2 and ~ 20 μm thickness were painted on the CaSiO_3 or Ca_2SiO_4 pellets and fired at respectively 1000 and 1200 °C for 24 h in air and in reducing atmosphere ($p_{\text{O}_2} \sim 10^{-6}$ atm). The average heating and cooling rates of the samples were 200 °C/h. In an actual membrane reactor, the

Table 1. Phases Observed by EDS and/or XRD in $\text{La}_{1-x}(\text{Ca}/\text{Sr})_x\text{CoO}_3/\text{CaSiO}_3$ and $\text{La}_{1-x}(\text{Ca},\text{Sr})_x\text{CoO}_3/\text{Ca}_2\text{SiO}_4$ Powder Mixtures Fired in Air and in Reducing Atmosphere (N_2) at 1000–1200 °C^a

system	x	mol % LMC	observed phases
$\text{La}_{1-x}\text{Ca}_x\text{CoO}_3/\text{CaSiO}_3$	0	17	$\text{Ca}_2\text{CoSi}_2\text{O}_7$ $\text{Ca}_3\text{Si}_2\text{O}_7$ (ss) (traces) $\text{Ca}_3\text{La}_6(\text{SiO}_4)_6$
	0	32	$\text{Ca}_3\text{La}_6(\text{SiO}_4)_6$ Ca_2SiO_4 CoO
	0.5	37	Ca_2SiO_4 $\text{Ca}_2\text{La}_6(\text{SiO}_4)_6$ CoO
$\text{La}_{1-x}\text{Ca}_x\text{CoO}_3/\text{Ca}_2\text{SiO}_4$	0	41	$\text{La}_{1-x}\text{Ca}_x\text{CoO}_3(\text{air})/$ $(\text{La},\text{Ca})_2\text{CoO}_4(\text{N}_2)$ Ca_2SiO_4 CaO(air)/CoO(?) (N_2) $\text{Ca}_2\text{La}_6(\text{SiO}_4)_6\text{O}_c$ (?)
	0.5	47	$\text{La}_{1-x}\text{Ca}_x\text{CoO}_3(\text{air})/$ $(\text{La},\text{Ca})_2\text{CoO}_4(\text{N}_2)$ Ca_2SiO_4 CoO Ca_3SiO_5 (?)
$\text{La}_{1-x}\text{Sr}_x\text{CoO}_3/\text{CaSiO}_3$	0.5	35	$\text{Sr}_{1-g}\text{La}_g\text{CoO}_3$ $(\text{Ca},\text{Sr})_a\text{La}_b(\text{SiO}_4)_6$ $(\text{Ca},\text{Sr})_2\text{SiO}_4$ CoO (traces)
$\text{La}_{1-x}\text{Sr}_x\text{CoO}_3/\text{Ca}_2\text{SiO}_4$	0.5	44	$\text{La}_{1-x}\text{Sr}_x\text{CoO}_3$ $(\text{Ca},\text{Sr})_2\text{SiO}_4$ CoO (traces)

^a The XRD spectra also revealed small unidentified diffraction peaks. The solid solution is assumed to appear between the $\text{Ca}_3\text{Si}_2\text{O}_7$ and $\text{La}_2\text{Si}_2\text{O}_7$ disilicates due to quite similar crystal structures. It should be noted that the metasilicate is excess in CaO relative to stoichiometric CaSiO_3 . Hence, there is an uncertainty in the mol % LMC given in the table of ~ 10 mol %. It should also be noted that some of the observed phases are nonequilibrium phases. The ? indicates possible traces of a phase observed by XRD.

perovskite should be used as a dense material and the sealing material will be painted on it.

The heat-treated powder mixtures and diffusion couples were subjected to XRD (Siemens D5005) using Cu K α radiation and a scan rate of 0.05°/s. The development of the microstructure of the samples was studied by scanning electron microscopy (SEM) (Zeiss DSM 940) and transmission electron microscopy (TEM) (Philips CM30, 300 kV) both equipped with energy dispersive spectroscopy (EDS) systems for microanalysis. Specimens for EDS linescans (SEM) were prepared from diffusion couples by dimpling from the perovskite side a sphere-cap with radius ~ 2 mm. The distance from the interface was calculated from the known profile of the sphere cap. Samples for TEM analysis were prepared by sectioning, polishing, and Ar-ion beam thinning.

3. Results

3.1. Powder Mixtures. Powder mixtures of LMC and CaSiO_3 or Ca_2SiO_4 were fired for 48–72 h at 1000–1200 °C to obtain information about coexistent phases in the $\text{CaO}-\text{La}_2\text{O}_3-\text{CoO}-\text{SiO}_2$ system. The observed phases in the different powder mixtures are summarized in Table 1. It should be noted that, in all the analyzed samples, the perovskite phase is deficient on a molar basis relative to CaSiO_3 or Ca_2SiO_4 . It should also be noted that the metasilicate is excess in CaO relative to stoichiometric CaSiO_3 .

In the $\text{LaCoO}_3/\text{CaSiO}_3$ powder mixtures with the lowest content of LCC, the observed phases correspond to a mixture of disilicates and orthosilicate (Table 1). Both LaCoO_3 and CaSiO_3 have been consumed in the

(9) The powders were prepared by Rita Glenne at Norsk Hydro a.s. Research Centre in Porsgrunn, Norway.

(10) Taylor, H. *Cement Chemistry*; Academic Press: London, U.K., 1990; p 15–22.

reaction between the two primary phases. With increasing amounts of LCC, the amount of orthosilicate increases at the expense of disilicates. The experimental results show that Co is present as the disilicate Ca₂-CoSi₂O₇ and CoO (Table 1, 17 and 32 mol % LaCoO₃). CoO is observed to be stable when Ca₂CoSi₂O₇ is not present. The effect of Ca substitution in the perovskite ($x = 0.5$) is an increasing amount of the orthosilicate phase Ca₂SiO₄ at the expense of the Ca₃La₆(SiO₄)₆ orthosilicate (Table 1). Firing these powder mixtures in reducing atmosphere ($p_{O_2} \sim 10^{-6}$ atm) gives coexistent phases that are indifferent from results obtained in air. This result is expected as all phases are insensitive to the partial pressure of oxygen in a wide p_{O_2} range. CoO decomposes to Co metal at $p_{O_2} \sim 10^{-12}$ atm at 1000 °C.¹¹

In the La_{1-x}Ca_xCoO₃ (LCC)/Ca₂SiO₄ powder mixtures the primary phases remained stable after firing at 1200 °C. The main secondary phases were CaO ($x = 0$) and CoO ($x = 0.5$) (Table 1). In addition, XRD revealed possible traces of the oxyorthosilicate phases Ca_aLa_b(SiO₄)₆O_c ($2a + 3b = 24 + 2c$) for LaCoO₃ and Ca₃SiO₅ for La_{0.5}Ca_{0.5}CoO₃. Figure 1a shows a SEM backscatter electron (BSE) image of the powder mixture of La_{0.5}Ca_{0.5}CoO₃/Ca₂SiO₄ after firing for 72 h at 1200 °C in air. Grains of CoO are clearly seen, but the perovskite and Ca₂SiO₄ are still the major phases after the firing.

Firing LCC/Ca₂SiO₄ powder mixtures in reducing atmosphere (Table 1) results in a complete transformation of the perovskite phase into La₂CoO₄, or more specifically (La_{1-x}Ca_x)₂CoO₄. The decomposition of the perovskite phase is accompanied by precipitation of CoO. Formation of small amounts of Ca-La oxyorthosilicates is also evident from XRD analysis. Figure 1b shows the microstructure of a powder mixture of La_{0.5}Ca_{0.5}CoO₃/Ca₂SiO₄ after firing for 72 h at 1200 °C in reducing atmosphere, and the CoO is clearly seen.

In the Sr-substituted systems, Sr_{1-q}La_qCoO₃ was the only phase differing from the secondary phases formed in the LCC/CaSiO₃/Ca₂SiO₄ systems (Table 1). When Sr_{1-q}La_qCoO₃ is present, the amount of CoO is reduced compared to the Ca-substituted powder mixtures.

3.2. Diffusion Couples. *3.2.1. La_{1-x}(Ca,Sr)_xCoO₃/CaSiO₃.* SEM backscatter images of selected diffusion couples of metasilicate and perovskite fired in air for 24 h at 1000 °C are given in Figure 2. The porous perovskite phase is seen on the left-hand side of the samples and layers of secondary phases are formed between the perovskite and the primary metasilicate. Note that the Ca₂SiO₄ inclusions shown in Figure 3b were present in the CaSiO₃ layer prior to the experiments and are not due to any reactions. The numbers of and the thickness of layers of secondary phases are higher for Ca- or Sr-substituted LaCoO₃ than for pure LaCoO₃. A summary of the formation of secondary phases is given in Table 2. In the LaCoO₃/CaSiO₃ diffusion couple only a thin layer (~1 μm) and some minor traces of secondary phases were detected (Figure 2a). The thin layer is rich in La, Ca, and Si (Table 2). XRD and EDS reveals a Ca-La silicate phase, Ca₃La₆(SiO₄)₆, with an apatite type of structure.¹² The other minor secondary phase was identified to be Ca₂CoSi₂O₇.

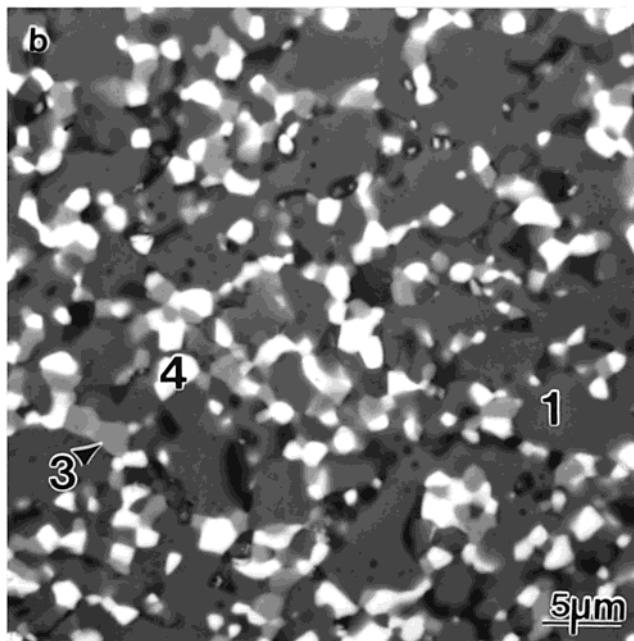
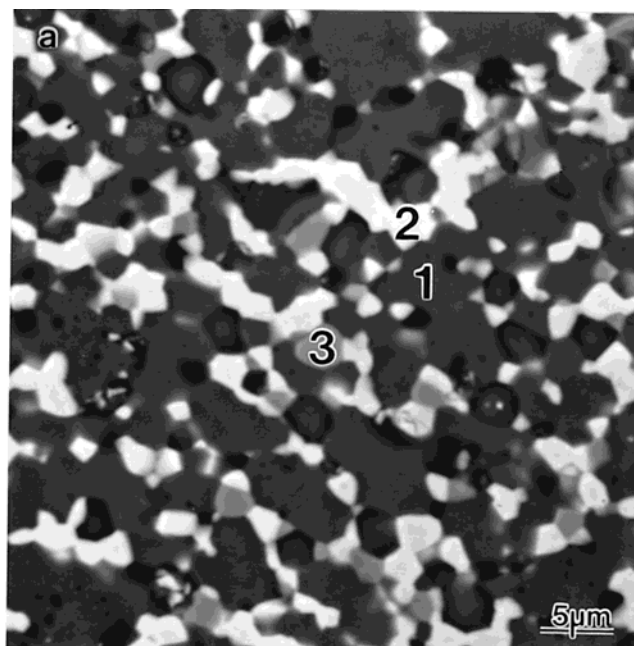


Figure 1. SEM backscatter images of (a) La_{0.5}Ca_{0.5}CoO₃/Ca₂SiO₄ powder mixture (47 mol % LMC) fired in air for 72 h at 1200 °C and (b) La_{0.5}Ca_{0.5}CoO₃/Ca₂SiO₄ powder mixture (47 mol % LMC) fired in reducing atmosphere ($p_{O_2} \sim 10^{-6}$ atm) for 72 h at 1200 °C. (1) = Ca₂SiO₄, (2) = LMC, (3) = CoO/Co₃O₄, (4) = (La,Ca)₂CoO₄.

The chemical composition of the CaSiO₃ phase after reaction with LaCoO₃ is close to the nominal composition. Due to the relatively low reaction temperature (1000 °C), the LaCoO₃ layer has not densified, giving rise to open porosity and a large surface area. The LaCoO₃ phase is found to contain some Ca and Si (4–6 cation %) based on EDS analysis. The reason for the Si/Ca content in the perovskite might be CaSiO₃ particles entering the porous perovskite layer during preparation of the SEM specimen.

In the LCC/CaSiO₃ diffusion couples, the formation of secondary phases are dependent on the Ca content

(11) Seppänen, M.; Kytö, M.; Taskinen, P. *Scand. J. of Metallurgy* **1979**, *8*, 199.

(12) McCarthy, G. J. *Proc. Rare Earth Res. Conf.*, **12th** **1976**, *2*, 665.

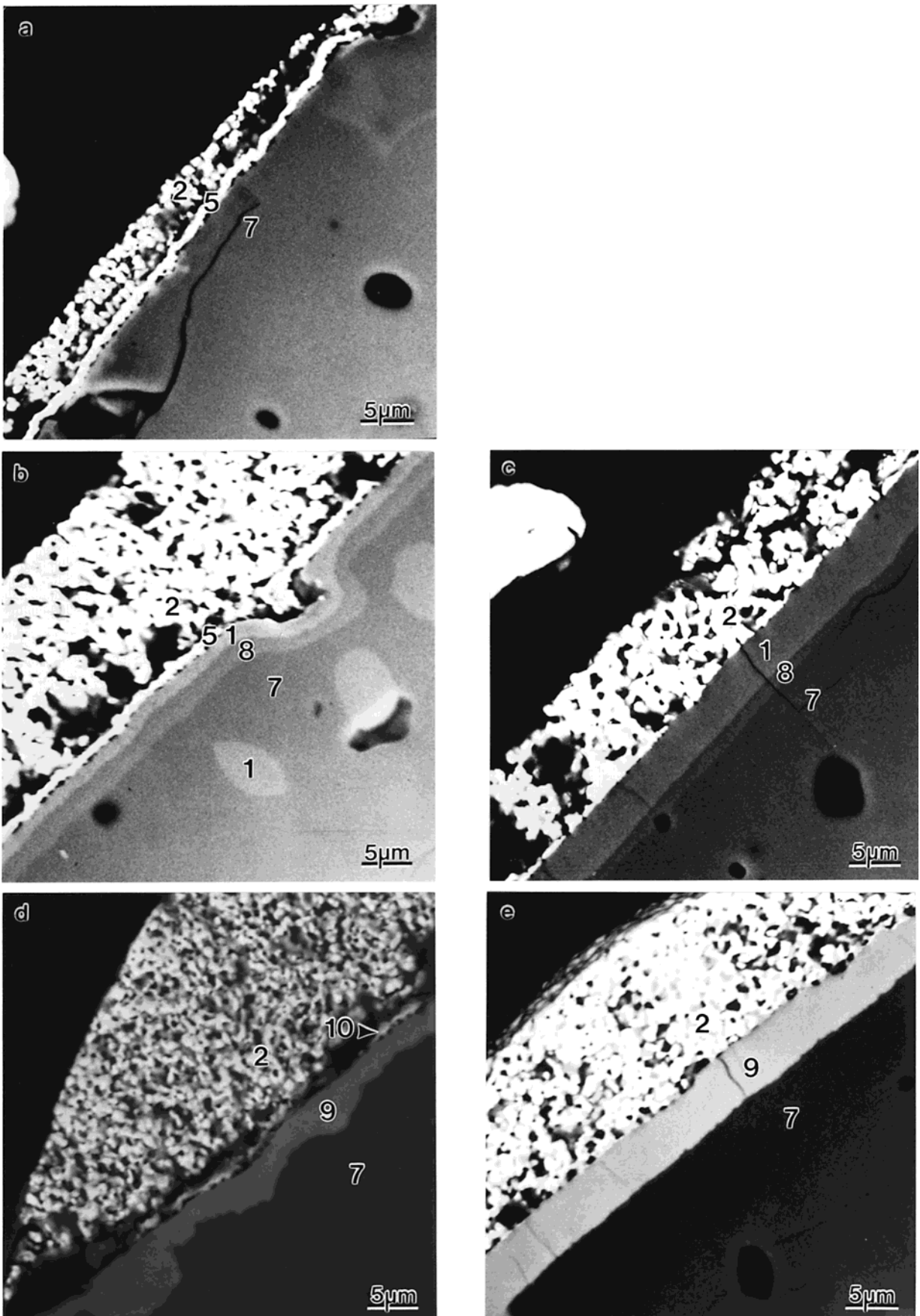


Figure 2. SEM backscatter images of (a) $\text{LaCoO}_3/\text{CaSiO}_3$, (b) $\text{La}_{0.8}\text{Ca}_{0.2}\text{CoO}_3/\text{CaSiO}_3$, (c) $\text{La}_{0.5}\text{Ca}_{0.5}\text{CoO}_3/\text{CaSiO}_3$, (d) $\text{La}_{0.8}\text{Sr}_{0.2}\text{CoO}_3/\text{CaSiO}_3$, and (e) $\text{La}_{0.5}\text{Sr}_{0.5}\text{CoO}_3/\text{CaSiO}_3$ diffusion couples fired for 24 h at 1000 °C. An intrinsic effect has caused precipitation of Ca_2SiO_4 grains in the CaSiO_3 matrix during heat treatment of the CaSiO_3 pellet in (b). (1) = Ca_2SiO_4 , (2) = LMC, (3) = $\text{CoO}/\text{Co}_3\text{O}_4$, (4) = $(\text{La},\text{Ca})_2\text{CoO}_4$, (5) = $\text{Ca}_a\text{La}_b(\text{SiO}_4)_6$, (6) = $\text{Ca}_2\text{CoSi}_2\text{O}_7$, (7) = CaSiO_3 , (8) = $\text{Ca}_3\text{Si}_2\text{O}_7$, (9) = $(\text{Ca},\text{Sr})_2\text{SiO}_4$, (10) = $(\text{Ca},\text{Sr})_a\text{La}_b(\text{SiO}_4)_6$.

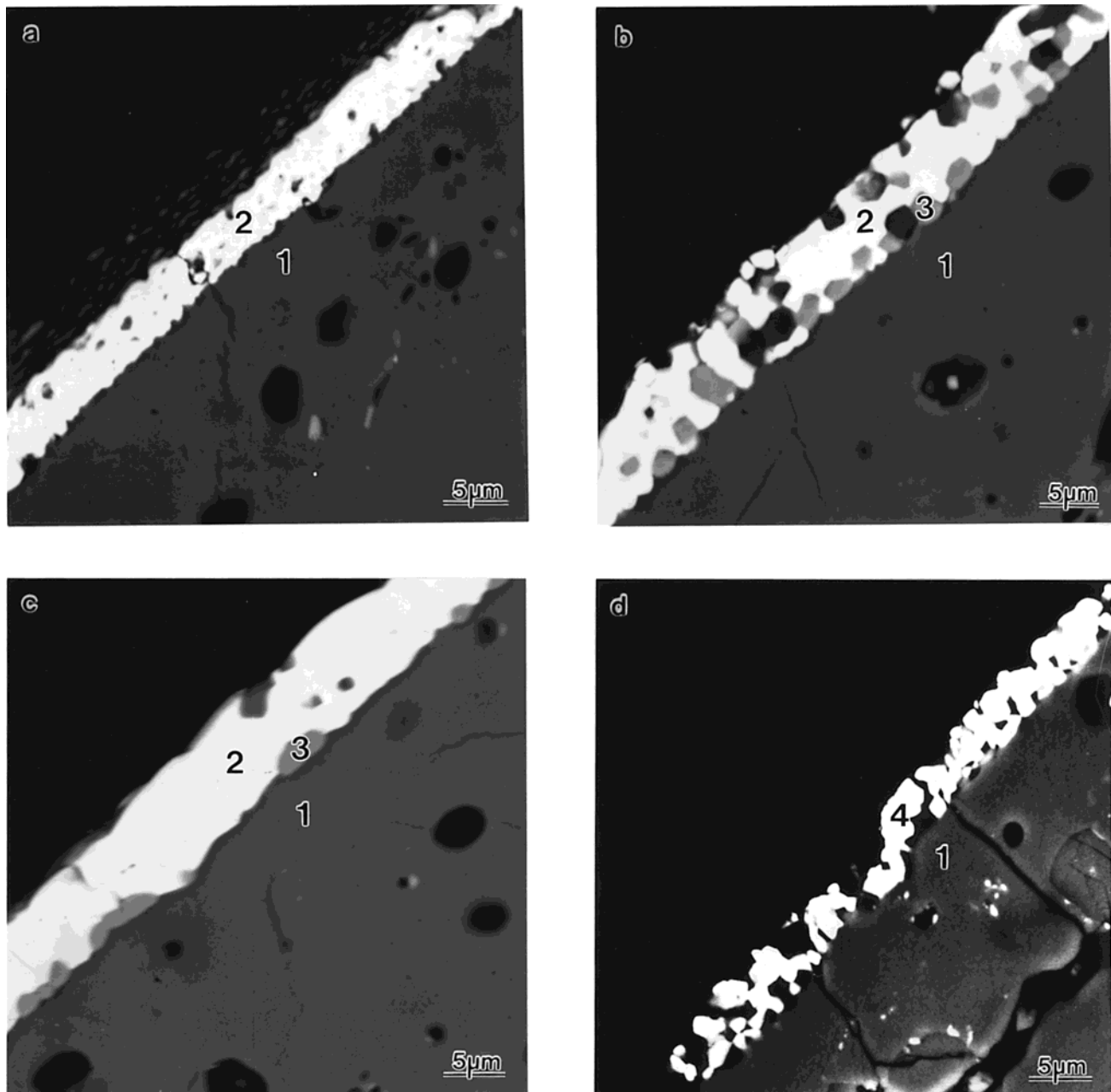


Figure 3. SEM backscatter images of (a) LaCoO₃/Ca₂SiO₄, (b) La_{0.5}Ca_{0.5}CoO₃/Ca₂SiO₄, and (c) La_{0.5}Sr_{0.5}CoO₃/Ca₂SiO₄ diffusion couples fired for 24 h at 1200 °C in air. Part (d) shows a La_{0.5}Ca_{0.5}CoO₃/Ca₂SiO₄ diffusion couple fired for 24 h at 1200 °C in reducing atmosphere ($p_{O_2} \sim 10^{-6}$ atm). The presence of small LMC particles at the Ca₂SiO₄ surface in (d) is due to specimen preparation. (1) = Ca₂SiO₄, (2) = LMC, (3) = CoO/Co₃O₄, (4) = (La,Ca)₂CoO₄.

in the LCC (x) (Figure 2b,c and Table 2). The major secondary phases are Ca₂SiO₄ and Ca₃Si₂O₇, which both were found to have approximately nominal composition after reaction with LCC. For $x = 0.5$, only these two secondary phases were detected. For $x = 0.2$, two additional secondary phases were detected (Table 2): a double orthosilicate with apatite structure and minor amounts of cobalt oxide. The ratio between the La and Ca content of the double orthosilicate was equal to 0.8, giving rise to a Ca₆La₄(SiO₄)₆ phase. The cobalt oxide was by XRD found to be a mixture of CoO and minor traces of Co₃O₄. The open porosity enabled partial oxidation of CoO to Co₃O₄ during cooling, explaining the presence of Co₃O₄. It should be noted that the sequence of the phases, LCC (with precipitates of CoO/Co₃O₄ ($x = 0.2$))–Ca₆La₄(SiO₄)₆ ($x = 0.2$)–Ca₂SiO₄–Ca₃Si₂O₇–Ca-

SiO₃, is equal for both $x = 0.2$ and 0.5. With increasing Ca content, the thickness of the Ca₂SiO₄ layer was found to increase at the expense of the Ca₃Si₂O₇ layer (Figure 2b,c). Inside the Ca₂SiO₄ layer for $x = 0.5$ (Figure 2c), perpendicular to the interface, tunnel cracking has occurred.¹³ The thermal expansion coefficient (TEC) of Ca₂SiO₄ is $39 \times 10^{-6} \text{ K}^{-1}$,^{14,15} the TEC of CaSiO₃ is $30 \times 10^{-6} \text{ K}^{-1}$,¹⁶ and the TEC of La_{0.5}Ca_{0.5}CoO₃ is $22.9 \times 10^{-6} \text{ K}^{-1}$.¹⁷ Thus, during cooling from the processing

(13) Hillman, C.; Suo, Z.; Lange, F. *J. Am. Ceram. Soc.* **1996**, 79, 8, 2127.

(14) Berman, R. G.; Brown, T. H. *Contrib. Mineral. Petrol.* **1985**, 89, 168.

(15) Berman, R. G.; Brown, T. H. *Contrib. Mineral. Petrol.* **1986**, 94, 262.

(16) Wang, Y. B.; Weidener, D. J.; Guyot, F. *J. Geophys. Res.-Solid Earth* **1996**, 0101, B1, 661.

Table 2. Survey of Secondary Phases Formed at $\text{La}_{1-x}(\text{Ca,Sr})_x\text{CoO}_3/\text{CaSiO}_3$ Interfaces in Diffusion Couples Fired for 24 h at 1000 °C^a

nominal x in $\text{La}_{1-x}\text{M}_x\text{CoO}_3$	M	secondary phases	thickness (μm)	rhombohedral angle, α_r , of $\text{La}_{1-x}\text{M}_x\text{CoO}_3$ (deg)		x in $\text{La}_{1-x}\text{M}_x\text{CoO}_3$	
				CaSiO_3	Ca_2SiO_4	CaSiO_3	Ca_2SiO_4
0.0		$\text{Ca}_3\text{La}_6(\text{SiO}_4)_6$	1	60.81 ± 0.03	60.74 ± 0.05	0.02	0.06
		$\text{Ca}_2\text{CoSi}_2\text{O}_7$	traces	60.79 ± 0.02	60.71 ± 0.02	0.03	0.08
0.2	Ca	CoO and Co_3O_4	traces				
		$\text{Ca}_6\text{La}_4(\text{SiO}_4)_6$	1				
		Ca_2SiO_4	2				
		$\text{Ca}_3\text{Si}_2\text{O}_7$	2.5				
0.5	Ca	Ca_2SiO_4	5	60.79 ± 0.02	~60	0.03	~0.50
		$\text{Ca}_3\text{Si}_2\text{O}_7$	2				
0.2	Sr	$\text{Sr}_a\text{La}_b(\text{SiO}_4)_6$	traces	60.81 ± 0.03	60.71 ± 0.02	0.02	0.08
		$(\text{Ca}_{0.63}\text{Sr}_{0.37})_2\text{SiO}_4$	3–4				
0.5	Sr	$(\text{Ca}_{0.44}\text{Sr}_{0.56})_2\text{SiO}_4$	5.5	60.71 ± 0.03	~60	0.08	~0.50

^a The phases have been observed by SEM and identified by EDS or XRD. Rhombohedral angle of $\text{La}_{1-x}\text{M}_x\text{CoO}_3$ after reaction with CaSiO_3 and Ca_2SiO_4 . The x in $\text{La}_{1-x}\text{M}_x\text{CoO}_3$ after reaction has been calculated by inserting into the linear fit, $\alpha_r = 60.8485 - 1.6724x$, of the rhombohedral angles of unreacted perovskite powders.

temperature, the Ca_2SiO_4 layer would shrink more due to its higher TEC and, due to strong interfaces, the Ca_2SiO_4 layer is constrained from shrinking, producing a biaxial, residual tensile stress in the embedded layer.

Backscattered electron images of the LSC/ CaSiO_3 diffusion couples are shown in Figure 2d,e, and a reaction layer of $(\text{Ca,Sr})_2\text{SiO}_4$ is observed. According to the SrO– SiO_2 phase diagram by Eskola,¹⁸ strontium disilicate does not exist. For $x = 0.2$, the $(\text{Ca,Sr})_2\text{SiO}_4$ layer is irregular, while for $x = 0.5$, the thickness is homogeneous (~5.5 μm). As expected, the Sr concentration of the $(\text{Ca,Sr})_2\text{SiO}_4$ layer is significantly higher for $x = 0.5$ than for $x = 0.2$ (Table 2). For $x = 0.2$, traces of a Sr–La silicate phase, $\text{Sr}_a\text{La}_b(\text{SiO}_4)_6$ ($2a + 3b = 24$), is formed. This phase is absent for $\text{La}_{0.5}\text{Sr}_{0.5}\text{CoO}_3$, as was the case for the Ca–La silicate phase for LCM. Tunnel cracking is also observed in the $\text{La}_{0.5}\text{Sr}_{0.5}\text{CoO}_3/\text{CaSiO}_3$ diffusion couple (Figure 2e). The CaSiO_3 phase is found to have approximately the nominal composition in diffusion couples with LSC.

Included in Table 2 is also the rhombohedral angle, α_r , of $\text{La}_{1-x}\text{M}_x\text{CoO}_3$ ($M = \text{Ca, Sr}$) after reaction with calcium metasilicate. The α_r angles of pure Ca- and Sr-substituted LaCoO_3 (before reaction) were found to decrease almost linearly with x ($\alpha_r = 60.862 - 1.6816x$ for Ca and $\alpha_r = 60.835 - 1.6632x$ for Sr) and become 60° at $x = 0.5$, demonstrating a phase transformation from rhombohedral to cubic at $x \approx 0.5$, in agreement with the data determined by Mineshige et al.¹⁹ After reaction with the metasilicate, the rhombohedral angles of the LMC phases are found to deviate from the α_r -values of the LMC powders before reaction, showing a change in Ca or Sr content during reaction. An estimate of the Ca(Sr) content in the perovskite after exposure to the silicates is also included in Table 2, showing a significant decrease in Ca(Sr) content for $x = 0.2$ and $x = 0.5$ after reaction with CaSiO_3 .

3.2.2. $\text{La}_{1-x}(\text{Ca,Sr})_x\text{CoO}_3/\text{Ca}_2\text{SiO}_4$. BSE images of selected LMC/ Ca_2SiO_4 diffusion couples fired in air or reducing atmosphere for 24 h at 1200 °C are shown in Figure 3. Due to the expected lower reactivity of the orthosilicate system compared to the metasilicate sys-

tem, the firing temperature was raised to 1200 °C. Despite the higher firing temperature, only small fragments of secondary phases evolved from the LMC phase were observed (Figure 3). For the $\text{LaCoO}_3/\text{Ca}_2\text{SiO}_4$ diffusion couple, SEM revealed no indications of secondary phases at the $\text{LaCoO}_3/\text{Ca}_2\text{SiO}_4$ interface (Figure 3a), but small (~0.1 μm) precipitates of CaO were detected by TEM in LaCoO_3 .

Also, in the $\text{La}_{1-x}(\text{Ca,Sr})_x\text{CoO}_3/\text{Ca}_2\text{SiO}_4$ diffusion couples there were no reaction layers at the interface, only precipitates of cobalt oxide (Figure 3b,c). The cobalt oxide was also here found to be a mixture of CoO and Co_3O_4 . Although the LMC phase has sintered at 1200 °C, the remaining open porosity enables partial oxidation of CoO during cooling.

Compared to the metasilicate system, the enhanced rhombohedral distortion of LMC is less significant after reaction with orthosilicate (Table 2). The composition of the perovskite is, hence, not altered much due to the interface reaction. For 50 mol % Ca or Sr in the perovskite prior to reaction, only a slight distortion of the cubic structure was observed by XRD after reaction with Ca_2SiO_4 .

The chemical composition of Ca_2SiO_4 after reaction was close to the nominal composition for all compositions studied. The measured diffusion profiles of La and Co into the Ca_2SiO_4 from LaCoO_3 are presented in Figure 4. From these data the diffusion coefficients of La and Co in Ca_2SiO_4 were estimated, assuming only unidirectional diffusion to occur. The boundary, $y = 0$, was maintained at constant concentration, c_0 , i.e., the solubility limit of La_2O_3 or cobalt oxide in Ca_2SiO_4 . If the diffusion constants, D_{La} and D_{Co} , are constant in the diffusion zone, then the solution to the diffusion equation is given as

$$c(y,t) = c_0 \operatorname{erfc}\left(\frac{y}{2\sqrt{Dt}}\right) \quad (1)$$

where $c(y,t)$ is the concentration at distance y and annealing time t .²⁰ Thus, eq 1 enables the calculation of an approximate value of the diffusion coefficient. The fit of eq 1 to the La and Co data shown in Figure 4 gives

(17) Menon, M. Private communication.

(18) Eskola, P. *Am. J. Sci. 5th Ser.* **1922**, 4, 336.

(19) Mineshige, A.; Inaba, M.; Yao, T.; Ogumi, Z.; Kikuchi, K.; Kawase, M. *J. Solid State Chem.* **1996**, 121, 423.

(20) Carslaw, H. S.; Jaeger, J. C. *Conduction of Heat in Solid*; Oxford University Press: Oxford, 1959; p 60.

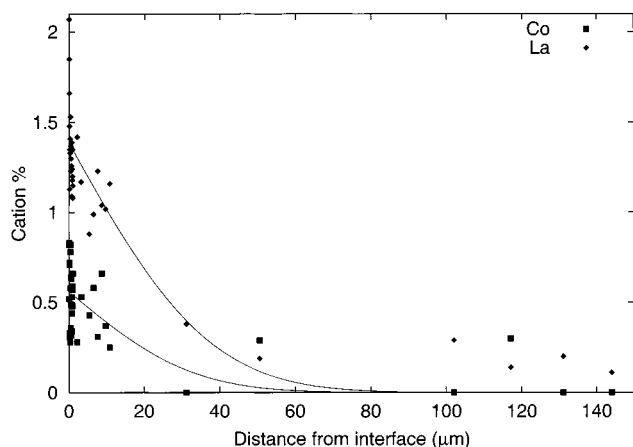


Figure 4. Diffusion profiles of La and Co into Ca₂SiO₄ from LaCoO₃. The fit of eq 1 to the data is given by the curves. The standard deviations in the measurements are ± 1 cation %.

diffusion coefficients on the order 10^{-15} m²/s and 10^{-16} m²/s, respectively.

The effect of the partial pressure of oxygen was studied by firing LCC/Ca₂SiO₄ diffusion couples in reducing atmosphere for 24 h at 1200 °C (Figure 3d). Due to the low partial pressure of oxygen, the perovskite phase has transformed completely into La₂CoO₄, or more specifically, (La_{1-x}Ca_x)₂CoO₄, as was observed for the powder mixtures. There was no indication of other secondary phases in the diffusion couples fired in reducing atmosphere, except for expected minor amounts of CoO. Due to the Ca content of the tetragonal La₂CoO₄ phase, the unit cell volume is smaller than for pure La₂CoO₄ ($V = 191.57 \text{ \AA}^3$).²¹ For 20 mol % Ca in the reacting perovskite, $V = 181.11 \text{ \AA}^3$, and for 50 mol % Ca in the reacting perovskite, $V = 179.90 \text{ \AA}^3$. The unit cell contraction of the (La_{1-x}(Ca,Sr)_x)₂CoO₄ phase is explained by the increase of the Co³⁺ content ($r = 0.61 \text{ \AA}$)²² at the expense of the Co²⁺ content ($r = 0.65 \text{ \AA}$)²² due to the presence of divalent ions, Ca²⁺ and/or Sr²⁺, at the La site.

4. Discussion

4.1. Coexistent Phases in the CaO/SrO–La₂O₃–CoO–SiO₂ System. According to Gibbs phase rule, the maximum number of coexistent condensed phases in the CaO–La₂O₃–CoO–SiO₂ system at given temperature and pressure is four. In powder mixtures with orthosilicate, the number of observed phases is always four (Table 1). For LaCoO₃/CaSiO₃ powder mixtures the number of observed phases is three (Table 1). The free variable is the composition of the solid solutions. In the system including SrO, the maximum number of coexistent condensed phases is five, but only orthosilicates are observed, and the constant molar ratio between oxygen and silicon removes one of the degrees of freedom. The SrO-containing system has therefore a maximum of one degree of freedom corresponding to the chemical composition of the solid solutions.

Formation of ternary oxides, A_xB_yO_z (A = acid, B = base, O = oxygen), can be identified as reactions

between acidic and basic binary oxides. In the quaternary CaO/SrO–La₂O₃–CoO–SiO₂ system, CoO and SiO₂ are acidic oxides, while CaO, SrO, and La₂O₃ are basic oxides according to Smith.²³ In the following discussion we will see that SiO₂ is the strongest acid leading to the formation of CoO. (In LaCoO₃/Ca₂SiO₄ CaO is formed.) In silicates, an increasing amount of basic oxides will give rise to various types of structures, ranging from infinite three-dimensional frameworks, as in silica itself (SiO₂), to isolated SiO₄⁴⁻ tetrahedra in orthosilicates such as Ca₂SiO₄. The important factor in relating formula to structure type is the oxygen-to-silicon ratio: for metasilicates, O/Si = 3; for disilicates, O/Si = 3.5; for orthosilicates, O/Si = 4; and for oxyorthosilicates, O/Si > 4. Silicate phases with different O:Si ratio may not be coexistent and will react into a phase with an intermediate O:Si ratio. Thus, metasilicates can only be coexistent with disilicates if they are stable. Disilicates may coexist with both meta- and orthosilicates, and orthosilicates may coexist with both di- and oxyorthosilicates.

The observed phases in the powder experiments can be understood in terms of chemical reactions (Table 3). The reaction at high metasilicate content ($0 < \text{mol \% LaCoO}_3 < 17$) in the system CaSiO₃–LaCoO₃ is given by reaction 1. Thus, the equilibrium phase composition corresponds to a mixture of disilicates and metasilicate. The space groups of Ca₃Si₂O₇ and La₂Si₂O₇ are respectively *P21/a* and *P21/c*, and a solid solution of these two disilicates is anticipated. Ca₂CoSi₂O₇ and Ca₃Si₂O₇ are coexisting phases according to Mukhopadhyay and Jacob,²⁴ in agreement with the present findings (Table 1, 17 mol % LaCoO₃).

On the basis of the CaO–CoO–SiO₂ phase diagram,²⁴ Ca₂CoSi₂O₇ should convert to CaCoSiO₄ and Ca₃Si₂O₇ with increasing amount of LaCoO₃. The phases formed in the composition region reaction $17 < \text{mol \% LaCoO}_3 < 20$ are given by reaction 2a. At 20 mol % LaCoO₃, the proposed total reaction is given by reaction 2b. (By total reaction we mean the reaction between the starting phases CaSiO₃ and LaCoO₃.) At a higher molar ratio between LaCoO₃ and CaSiO₃ ($> 20 \text{ mol \%}$), CaCoSiO₄ is further converted to Ca₃Si₂O₇ and CoO according to reactions 3a and 3b.

At more than 25 mol % LaCoO₃, other orthosilicates are formed. Pure La₈(SiO₄)₆ is not stable below 1600 °C²⁵ and is therefore not stable at the temperatures in question here. The composition Ca₃La₆(SiO₄)₆ is suggested on the basis of the findings from the diffusion couples and is also in agreement with the compositions of orthosilicates reported by McCarthy.¹² Thus, orthosilicates are formed according to reactions 4a and 4b. Solid solution of the orthosilicates is expected on the basis of the Ca₂SiO₄–La₈(SiO₄)₆ phase diagram.²⁶ The phase composition along the CaSiO₃–LaCoO₃ line for $0 < \text{mol \% LaCoO}_3 < 40$ based on the reactions in Table 3 is shown in Figure 5.

At a higher LaCoO₃/CaSiO₃ ratio ($> 40 \text{ mol \% LaCoO}_3$), all disilicate has disappeared, and the perovskite,

(23) Smith, D. W. *J. Chem. Educ.* **1987**, *64*, 480.

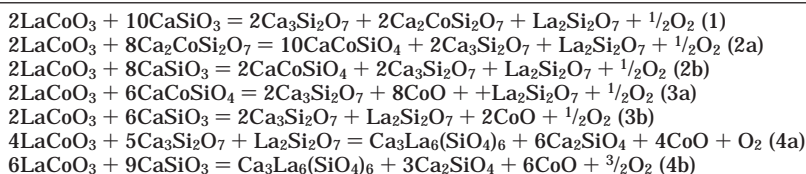
(24) Mukhopadhyay, S.; Jacob, K. *Am. Miner.* **1996**, *81*, 963.

(25) Toropov, N. A.; Bondar, I. A.; Galakhov, F. Y. *Izv. Akad. Nauk SSSR, Otd. Khim. Nauk* **1961**, *5*, 740.

(26) Toropov, N. A.; Fedorov, N. F. *Izv. Akad. Nauk SSSR, Neorg. Mater.* **1965**, *1*, 1, 126.

(21) Russ, J. J. *Inorg. Chem.* **1979**, *24*, 652.

(22) Shannon, R. D.; Prewitt, C. T. *Acta Crystallogr.* **1968**, *B25*, 925.

Table 3. Chemical Reactions in the Pseudobinary System CaSiO₃-LaCoO₃^a

^a The phases formed in the actual composition regions are given by reactions a; b denotes total reactions which are the reactions between the starting phases CaSiO₃ and LaCoO₃.

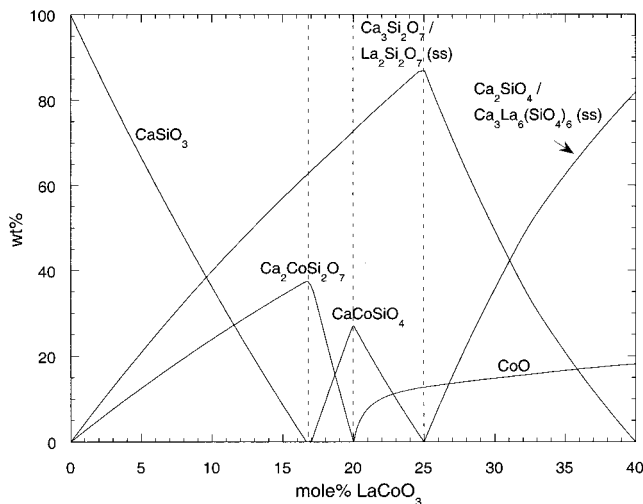


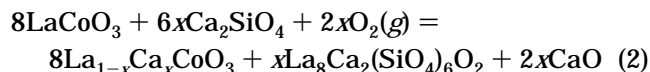
Figure 5. Estimated phase composition at 1000 °C along the line CaSiO₃-LaCoO₃ based on the chemical reactions given in Table 3. Note that the sharp edges on the curves are due to the composition changing from belonging to one ternary system to another. Solid solution is assumed to appear between the Ca₃Si₂O₇ and La₂Si₂O₇ disilicates and the Ca₂SiO₄ and Ca₃-La₆(SiO₄)₆ orthosilicates due to quite similar crystal structures.

La_{1-x}Ca_xCoO₃, appears in equilibrium with CoO and orthosilicates. The formation of the two orthosilicates and CoO are in agreement with the experimental findings (Table 1, 32 mol % LCC). At an even higher LaCoO₃ content the equilibration of the Ca/La ratio in the perovskite and orthosilicate will also cause the formation of oxyorthosilicate (e.g. La₈Ca₂(SiO₄)₆O₂). This oxyorthosilicate phase has an apatite structure, and solid solubility with La₃Ca₆(SiO₄)₆ is anticipated.

The effect of substituting Ca into LaCoO₃ is a displacement of the phase separation lines in the phase composition diagram to a higher perovskite:metasilicate ratio. The phases are the same as in Figure 5, except for a higher Ca:La ratio in the double orthosilicates and oxyorthosilicates. The observation of two orthosilicates and CoO in the La_{0.5}Ca_{0.5}CoO₃/CaSiO₃ powder mixture is in agreement with the proposed coexistent phases for >40 mol % LaCoO₃ in the CaSiO₃-LaCoO₃ system.

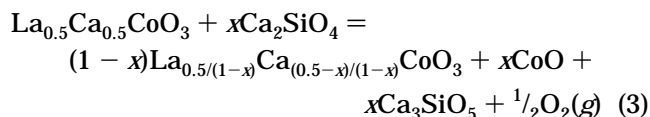
In the reaction between calcium orthosilicate and the perovskite (Table 1), the perovskite phase remains stable but changes composition on A site followed by precipitation of CaO for $x = 0$ and CoO for $x = 0.5$. In addition, small amounts of an oxyorthosilicate were formed, but we were not able to identify the composition.

According to the CaO-SiO₂-La₂O₃ phase diagram by McCarthy,¹² several oxyorthosilicates exist. However, La₈Ca₂(SiO₄)₆O₂ is satisfactorily documented (PDF card 29-337, ICDD 1999), giving rise to the reaction



neglecting the concentration of La in Ca₂SiO₄. The observed phases in the LaCoO₃/Ca₂SiO₄ system are in accordance with this equation (Table 1).

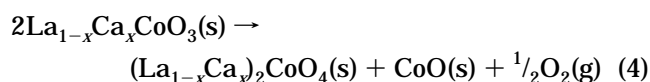
The observed reaction between calcium orthosilicate and La_{0.5}Ca_{0.5}CoO₃ is explained by the reaction



neglecting the concentration of La in Ca₂SiO₄. This reaction is reductive in nature as opposed to the reaction between LaCoO₃ and Ca₂SiO₄ (2), which is oxidative.

The chemical stability of a perovskite phase was observed to increase when Ca in LCC was substituted with Sr. This can be understood in relation to the phase equilibria in the pseudobinary systems CaO-CoO and SrO-CoO. According to the CaO-CoO phase diagram by Woermann and Muan²⁷ CaCoO_z does not exist, and above 1026 °C only CoO with divalent cobalt is stable. No phase diagram has been reported for the SrO-CoO system, but the perovskite-like phase SrCoO_{3-δ} is known to be stable above about 900 °C.²⁸ In the LSC/CaSiO₃ powder mixture significant amounts of Sr_{1-q}La_qCoO_{3-δ} is formed, revealing an increased thermodynamic stability of a perovskite phase with Sr substitution. In addition to the perovskite-like phase, orthosilicate and possible traces of CoO are formed. Extensive solid solution is observed both for the single and double orthosilicates, respectively (Ca,Sr)₂SiO₄ and (Ca,Sr)_aLa_b(SiO₄)₆, in accordance with the similarities in the crystal structure of Ca- and Sr-orthosilicates. The reaction between LSC and Ca₂SiO₄ is explained by a reaction like (3), including the solid solubility of Sr₂-SiO₄ in Ca₂SiO₄ and Sr₃SiO₅ in Ca₃SiO₅.

According to the phase diagram at 1127 °C given by Petrov et al.,²⁹ the stable phases of the La-Co-O system for $0 > \log(p_{\text{O}_2}) > 10^{-5}$ atm are La₂CoO₄ and CoO. After firing LCC/Ca₂SiO₄ powder mixtures in reducing atmosphere, the perovskite was observed to be completely converted into La₂CoO₄ or more specifically (La_{1-x}Ca_x)₂CoO₄ according to the following reaction



(27) Woermann, E.; Muan, A. *J. Inorg. Nucl. Chem.* **1970**, *32*, 5, 1457.

(28) Vashook, V. V.; Zinkevich, M. V.; Ullmann, H.; Paulsen, J.; Trofimenko, N.; Teske, K. *Solid State Ionics* **1997**, *99*, 23.

(29) Petrov, A. N.; Cherepanov, V. A.; Zuyev, A. Y.; Zhukovsky, V. M. *J. Solid State Chem.* **1988**, *77*, 1.

Here we have assumed stoichiometric oxygen contents for all compounds and no change of the La/Ca ratio in the two lanthanum cobalt oxide phases. The decomposition of the perovskite phase is accompanied by precipitation of CoO. Thus, the coexistent phases at equilibrium in the LCC/Ca₂SiO₄ system in reducing atmosphere are (La_{1-x}Ca_x)₂CoO₄, Ca₂SiO₄, CoO, and oxyorthosilicate.

4.2. Kinetics and Reaction Mechanisms in Diffusion Couples. *4.2.1. La_{1-x}(Ca,Sr)_xCoO₃/CaSiO₃.* The estimated compositions of the perovskite layers (Table 2) imply that the reaction between LMC and CaSiO₃ will continue as long as there is Ca or Sr left in the perovskite, unless the reaction is limited by diffusion due to the increasing thickness of the reaction layers. Thus, compared to the La_{1-x}Ca_xMnO₃/ZrO₂(CaO) system, where a minimum in reactivity was observed for $x \approx 0.3$,³⁰ the LMC/CaSiO₃ has no such minimum. According to Smith,²³ the acidity parameter of SiO₂ and ZrO₂ are respectively 0.9 and 0.1. [An acidity scale has been proposed in which the difference in the acidity parameters ($a_B - a_A$), of a metal oxide and a non-metal oxide is the square root of the enthalpy of reaction of the acid and base.] Hence, the acidity of SiO₂ is high enough to cause a total extraction of basic oxides from the perovskite phase and, thus, decomposition of the perovskite structure, giving rise to LaCoO₃/CaSiO₃ as the kinetically most stable interface.

The experimentally observed sequence of the different secondary phases in the LCC/CaSiO₃ diffusion couples was (1) Ca₃Si₂O₇, (2) Ca₂SiO₄, and (3) Ca_aLa_b(SiO₄)₆, starting from the CaSiO₃ side. This sequence shows as expected a change from metasilicate to disilicate and orthosilicate. The three secondary phases are expected to be formed in the same order as given above, due to the relative diffusion rates. Basic oxides, such as CaO, easily diffuse from the perovskite to CaSiO₃, forming Ca₃Si₂O₇ and then Ca₂SiO₄, because of their high affinities for silicon oxide. The reaction mechanism continues with simultaneous diffusion of Ca²⁺ and O²⁻ across the orthosilicate and disilicate phases.³¹ The available data on diffusion of Si suggest low mobility in orthosilicates,³²⁻³⁴ in accordance with the fact that it is bonded to four oxygen ions. Thus, disilicate forms at the Ca₃Si₂O₇/CaSiO₃ interface and orthosilicate forms at the Ca₂SiO₄/Ca₃Si₂O₇ interface. Subsequent formation of Ca_aLa_b(SiO₄)₆ is due to diffusion of La ions into the Ca₂SiO₄ phase. Ca_aLa_b(SiO₄)₆ was observed to be present for $x = 0.2$ but absent for $x = 0.5$. The reason for Ca_aLa_b(SiO₄)₆ formation for $x = 0.2$ is that the extensive formation of orthosilicate and disilicate empties the perovskite phase for Ca (Table 2). This was also the case for the LaCoO₃/CaSiO₃ interface.

Since the LSC ($x = 0.5$)/CaSiO₃ system only revealed (Ca,Sr)₂SiO₄ as a secondary phase, this system was used to calculate the transport coefficient for the formation of the secondary phase. If the rate of (Ca,Sr)₂SiO₄

formation is limited by solid-state diffusion through the (Ca,Sr)₂SiO₄ layer, the thickness, x , of the newly formed phase might obey the parabolic rate law

$$x^2 = 2k_p t \quad (5)$$

where t is time and k_p is a transport coefficient related to solid-state diffusion.³¹ The transport rate coefficient thus calculated is on the order of 10⁻¹⁶ m²/s at 1000 °C. Horita et al.^{2,3} studied reaction of SOFC components with sealing materials and found that for the reaction between YSZ and Pyrex glass the transport rate coefficient for formation of ZrSiO₄ at the interface was on the order of 10⁻¹⁶ m²/s at 1200 °C and 10⁻¹⁷ m²/s at 1000 °C. Hence, the La_{0.5}Sr_{0.5}CoO₃/CaSiO₃ system is slightly more reactive than the YSZ/Pyrex glass system.

4.2.2. La_{1-x}(Ca,Sr)_xCoO₃/Ca₂SiO₄. In the La_{1-x}(Ca,Sr)_xCoO₃/Ca₂SiO₄ diffusion couples there were no reaction layers at the interface; only small fragments of secondary phases evolved from the LMC phase were observed. Thus, the LMC/Ca₂SiO₄ system has a significantly higher kinetic and thermodynamic stability compared to the LMC/CaSiO₃ system.

The chemical composition of Ca₂SiO₄ after the reaction with LMC was found to be close to the nominal composition, and the diffusion coefficients of La and Co were calculated to be on the order of 10⁻¹⁵ and 10⁻¹⁶ m²/s, respectively. Thus, La and Co have relatively low mobilities in Ca₂SiO₄.

The experimental findings on the metasilicate and orthosilicate systems demonstrate that the O:Si ratio is an excellent indicator of the stability of calcium silicates against LMC. The observed decomposition of the perovskite structure in the metasilicate case demonstrates that the activity of SiO₂ is too high to allow it to coexist with LMC. Orthosilicate, on the other hand, has a lower SiO₂ activity, allowing it to coexist with the perovskite. Thus, the stability of the membrane/sealant interface is quite sensitive to the O:Si ratio of the calcium silicate: $3 < O/Si < 4$ (closer to 4) gives rise to good sealing properties and moderate reactivity to the membrane material. A suitable sealing material is a two-phase material, e.g. an orthosilicate glass-ceramic material with small amounts of metasilicate or disilicate glass.

5. Conclusions

The reaction between Ca- and Sr-substituted LaCoO₃ and calcium silicate glass-ceramics (CaSiO₃ and Ca₂-SiO₄) has been investigated. The phase composition along the composition line CaSiO₃-LaCoO₃ has been worked out, and reaction mechanisms for diffusion couples have been discussed. Pure LaCoO₃ was found to be kinetically more stable to both CaSiO₃ and Ca₂-SiO₄ than Ca- and Sr-substituted LaCoO₃. CaSiO₃ turned out to have the best sealing properties due to a significant amount of glass phase. However, the high reactivity of the LMC/CaSiO₃ system rules out CaSiO₃ as a suitable sealant. Several layers of secondary phases with different thermal expansion were formed, causing tunnel cracking. Ca₂SiO₄ turned out to give the most chemically stable interface to LMC. No layered reaction products were observed either in air or in reducing atmosphere. Hence, the O:Si ratio is an indicator of the

(30) Faaland, S.; Einarsrud, M.-A.; Wiik, K.; Høier, R.; Grande, T. *J. Mater. Sci.* **1999**, *34*, 957.

(31) Schmalzried, H. *Chemical Kinetics of Solids*; VCH: Weinheim, 1995; p 153.

(32) Jaoul, O. *Earth Planet Sci. Lett.* **1980**, *47*, 391.

(33) Jaoul, O. *Anelasticity in the Earth*; Am. Geophys. Union: Washington, 1981; p 95.

(34) Houlier, B. *Phys. Earth Planet. Inter.* **1988**, *50*, 240.

stability of the membrane/sealant interface. However, the sealing properties of Ca_2SiO_4 are poor, because the material crystallizes completely. Everything taken into consideration, a suitable calcium silicate sealing material is a two-phase material with $3 < \text{O/Si} < 4$ (closer to 4), having good sealing properties and moderate reactivity to the dense membrane material.

Acknowledgment. The authors are grateful to the Norwegian scientific foundation VISTA for their financial support and to Rita Glenne at Norsk Hydro Research Center in Porsgrunn, Norway, for preparing the perovskite powders.

CM991184N